Ultrasonic Motor Control Based on Recurrent Fuzzy Neural Network Controller and General Regression Neural Network Controller

Tien-Chi Chen[1], Tsai-Jiun Ren[2], and Yi-Wei Lou[1]

[1] Department of Electrical Engineering, Kun Shan University, Tainan, Taiwan
tchichen@mail.ksu.edu.tw
[2] Department of Information Engineering, Kun Shan University, Tainan, Taiwan
cyrusren@mail.ksu.edu.tw

Abstract. The travelling-wave ultrasonic motor (TWUSM) has been used in industrial, medical, robotic and automotive applications. However, the TWUSM has the nonlinear characteristic and dead-zone problem which varies with many driving conditions. A novel control scheme, recurrent fuzzy neural network controller (RFNNC) and general regression neural network controller (GRNNC), for a TWUSM control is presented in this paper. The RFNNC provides real-time control such that the TWUSM output can tightly track the reference command. The adaptive updated RFNNC law is derived using Lyapunov theorem such that the system stability can be absolute. The GRNNC is appended to the RFNNC to compensate for the TWUSM dead-zone using a predefined set. The experimental results are shown to demonstrate the effectiveness of the proposed control scheme.

Keywords: Travelling-wave ultrasonic motor, TWUSM, Recurrent fuzzy neural network controller, RFNNC, Lyapunov theorem, General regression neural network controller, GRNNC, Dead-zone.

1 Introduction

The TWUSM is a new type of motor that is driven using the ultrasonic vibration force of piezoelectric elements. It has excellent performance and many useful features [1], such as high torque at low speed, quiet operation, light weight and compact size, quick response, wide velocity range, high efficiency, simple structure, easy production process and no electro-magnetic interference [2-3]. The TWUSM can be used in many industries such as industrial, medical, automotive, aerospace science and accurate positioning actuators [4].

The TWUSM is a new type of actuator with different control technique and operating principles than conventional electro-magnetic motors. Because the TWUSM is composed of piezoelectric ceramics instead of electro-magnetic windings in the motor structure [5], the TWUSM driving principles are based on the ultrasonic vibration of piezoelectric elements and mechanical frictional force [6].

The TWUSM motor dynamic model is very complicated with nonlinear characteristics, which vary with many driving conditions. The TWUSM parameters

K. Madani et al. (Eds.): *Computational Intelligence*, SCI 465, pp. 291–305.
DOI: 10.1007/978-3-642-35638-4_19

are nonlinear and time varying due to the increasing temperature and different motor drive operating conditions. These parameters include driving frequency, source voltage and load torque [1]. The TWUSM control characteristics are very complex to analyze and accurately model [7].

In general, the TWUSM drive and digital control system apply three independent control methods which are the drive frequency control, supplied voltage control and applied voltage phase difference control. In the phase difference control method the motor shows a variable dead-zone in the control input (phase difference of applied voltages) against the operating frequency. The dead-zone is due to a large static friction torque appearing at low speed. It is therefore difficult to design a perfect angle controller that can provide accurate control at all times. According to practical control issues, many speed controllers based on PI (proportional plus integral) controller using mathematical models of the motor have been reported.

Because the PI controller control algorithms are simple and the controllers have advantages such as high-stability margin and high-reliability when the controllers are tuned properly, the PI controller can be used to drive common motors. However, the PI controller cannot maintain these virtues at all times. The ultrasonic motor has nonlinear speed characteristics which vary with drive operating conditions. In order to overcome these difficulties, a dynamic controller with adjustable parameters and online learning algorithms is suggested for unknown or uncertain dynamic systems [8-9].

In the past few years there has been much research on neural network (NN) applications in order to deal with the nonlinearities and uncertainties in control systems [10-12]. According to NN structures, the NN can be classified mainly as feed-forward neural network (FNN) and recurrent neural network (RNN) [13]. It is well known that the FNN is capable of closely approximating continuous functions. The FNN conducts static mapping without the aid of delays. The FNN is unable to represent dynamic mapping. Although the FNN presented in much research is used to deal with delay and dynamic problems, The FNN requires a large number of neurons to express dynamic responses [14]. The weight calculations are not updated quickly and the function approximation is sensitive to the training data.

The RNN [15], on the other hand has superior capabilities compared to the FNN. The RNN exhibits dynamic response and information storing ability for later use. Since the recurrent neuron has an internal feedback loop, it captures the dynamic response of a system without external feedback through long delays. Thus, the RNN is a dynamic mapping and displays good control performance in the presence of unknowable and time-varying model dynamics [16]. As a result the RNN is better suited for dynamic systems than the FNN.

If the number of hidden neurons too many, the computation load becomes heavy so that the RNN is not suitable for online practical applications. If the number of hidden neurons is too few the learning performance may not be good enough to achieve the desired control performance. To solve this problem we propose a novel controller, the RFNNC, to maintain high accuracy.

The RFNNC has a number of attractive advantages compared to recurrent neural network control. For example, it has superior modelling performance due to local modelling and the fuzzy partition of the input space, linguistic dynamic fuzzy rule description, a learning based training example structure and parsimonious models with smaller parametric complexity [17]. The RFNNC combines fuzzy reasoning capability to handle uncertain information and the artificial recurrent neural network

capability to learn processes to deal with the nonlinearities and uncertainties that frustrate the TWUSM.

The RFNNC still presents a challenge considering the TWUSM as a plant. In the proposed RFNNC, the controller is effective in handling the small characteristic variations in the motor due to RFNNC connecting weight updating. However, the RFNNC is not able to fully compensate for the dead-zone effect and therefore the dynamic response deteriorates [18]. For these reasons an angle control scheme for the TWUSM with dead-zone compensation based on the RFNNC is presented in this research. The GRNNC is adopted to determine the dead-zone compensating input and decouple the RFNNC output. Because of the saturation reverse effect, phase difference control is not adequate for precise angle control. Therefore, the drive frequency must also be implemented, leading to a more accurate control strategy. The GRNNC based on RFNNC applies both the driving frequency and phase difference constructions as a dual-mode control method. The proposed controller can take the nonlinearity into account and compensate for the TWUSM dead zone. This approach also provides robust performance against parameter variations. The usefulness and validity of the proposed control scheme is examined through experimental results. The experimental results reveal that the GRNNC based on the RFNNC maintains stable performance under different motion conditions.

2 The Control Scheme

The TWUSM nonlinear dynamic system is expressed as:

$$\ddot{\theta} = f(\theta) + g(\theta)u(t) + d(t) \tag{1}$$

where $f(\cdot)$ and $g(\cdot)$ are unknown functions that are bounded. *u(t)* is the control input, *d(t)* is the external disturbance, and θ is rotor angle displacement of the TWUSM.

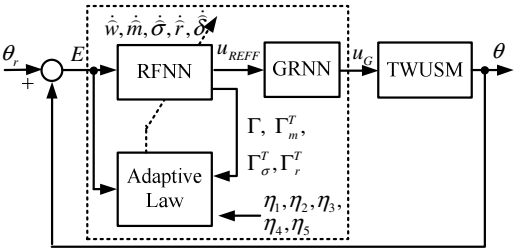

Fig. 1. The proposed control structure

The proposed control scheme, illustrated in Fig. 1, is composed of two main blocks, RFNNC and GRNNC. The RFNNC provides real-time control such that the TWUSM output can track the reference command θ_r. The back-propagation algorithm is applied in the RFNNC to automatically adjust the parameters on-line. The RFNNC adaptive laws are derived using the Lyapunov Theorem such that the system stability can be absolute. Γ, Γ_m^T, Γ_σ^T, Γ_r^T are the adaptive update law training

parameters and η_1, η_2, η_3, η_4, η_5 are the learning rates. The GRNNC is appended to the RFNNC to compensate for the TWUSM dead-zone using a predefined set. The GRNNC is designed to avoid the TWUSM dead-zone response.

2.1 Recurrent Fuzzy Neural Networks Controller

A controller is designed such that the TWUSM output can track the reference command. The tracking error vector is first defined as

$$E = \left[e,\ \dot{e}\right]^T \tag{2}$$

where $e = \theta_r - \theta$ is the angle tracking error. From (1) and (2), an ideal controller can be chosen as

$$u^*(t) = \frac{1}{g_n(\theta)}[\ddot{\theta}_r - f_n(\theta) - d_n(t) + K^T E] \tag{3}$$

where $K = \left[k_2, k_1\right]^T$, k_1 and k_2 are positive constants. Applying (2) to (3), the error dynamics can be expressed as

$$\ddot{e} + k_1\dot{e} + k_2 e = 0 \tag{4}$$

If K is chosen to correspond to Hurwitz polynomial coefficients, it is a polynomial whose roots lie strictly in the open left half of the complex plane. A result is then achieved where $\lim_{t\to\infty} e(t) = 0$ for any initial conditions. Nevertheless, the functions $f(\theta)$ and $g(\theta)$ are not accurately known and the external load disturbances are perturbed. The ideal controller $u^*(t)$ cannot thus be practically implemented. Therefore, the RFNNC will be designed to approximate this ideal controller.

Figure 2 shows the four-layer RFNNC structure, which is comprised of an input layer, membership layer, rule layer and output layer. The superscript of symbol y means the ordinal number of the layer, and the subscript of symbol y means its number. The symbol w expresses the weight of the signals. The RFNNC model is summarized as follows:

(1) Input Layer. The RFNNC inputs are $x_e^1 = e$ and $x_{\dot{e}}^1 = \dot{e}$. The input layer outputs are $y_{e,i}^1$ and $y_{\dot{e},i}^1$, which are equal to the inputs:

$$y_{e,i}^1 = x_e^1; \quad i = 1 \sim 3 \tag{5}$$

$$y_{\dot{e},i}^1 = x_{\dot{e}}^1; \quad i = 1 \sim 3 \tag{6}$$

(2) Membership Layer. There are three membership functions for e and $\dot{e}$, respectively. The three signals are sent to calculate the degree belonging to the specified fuzzy set. The outputs $y_{e,i}^2$ and $y_{\dot{e},i}^2$ are as follows:

$$y_{e,i}^2 = \exp\left(-\left(\frac{y_{e,i}^1 - m_{e,i}}{\sigma_{e,i}}\right)^2\right); \quad i = 1 \sim 3 \tag{7}$$

$$y_{\dot{e},j}^{2} = \exp\left(-\left(\frac{y_{\dot{e},j}^{1} - m_{\dot{e},j}}{\sigma_{\dot{e},j}} \right)^{2} \right); \quad i = 1 \sim 3 \tag{8}$$

where m and σ are the mean and standard deviation of the Gaussian function. They express different RFNNC membership functions so the layer output can represent the degree the input belongs to the fuzzy rule.

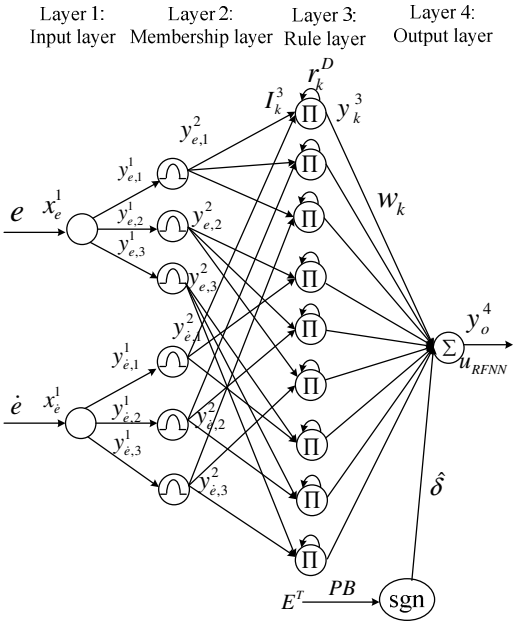

Fig. 2. The four-layer RFNNC structure

(3) Rule Layer. The outputs y_k^3 of the rule layer can be expressed as

$$y_k^3(t) = (1 + \frac{1}{1 + 100 \cdot \exp^{-10 r_k^D y_k^3(t-1)}}) y_{e,i}^2(t) y_{\dot{e},j}^2(t) \tag{9}$$

where $k = 3 \times (i-1) + j$, $i = 1 \sim 3$, $j = 1 \sim 3$ and $k = 1 \sim 9$. r_k^D are the weights. The value of y_k^3 is always positive and between zero and two.

(4) Output Layer. The output y_o^4 of the RFNNC can be expressed as

$$\begin{aligned} u_{RFNN} = y_o^4 &= \sum_{k=1}^{9} w_k y_k^3 + \hat{\delta} \mathrm{sgn}(\mathrm{E}^{\mathrm{T}} \mathrm{PB}) \\ &= w^T \Gamma(x, m, \sigma, r) + \hat{\delta} \mathrm{sgn}(\mathrm{E}^{\mathrm{T}} \mathrm{PB}) \end{aligned} \tag{10}$$

where $\Gamma(x, m, \sigma, r) = \begin{bmatrix} y_1^3 & y_2^3 & \cdots & y_9^3 \end{bmatrix}^T$ fuzzy rule function vector, and $w = \begin{bmatrix} w_1 & w_2 & \cdots & w_9 \end{bmatrix}^T$ adjustable output weight vector, δ a small positive constant, and $E = [e, \dot{e}]^T$.

Assume that an optimal RFNNC exists to approximate the ideal control law such that

$$u^* = u^*_{RFNN}(e, w^*, m^*, \sigma^*, r^*) + \varepsilon = w^{*T}\Gamma^* + \varepsilon \tag{11}$$

where ε is a minimum reconstructed error, w^*, m^*, σ^*, r^* and Γ^* are optimal parameters of w, m, σ, r and Γ, respectively. Thus, the RFNNC control law is assumed to take the following form:

$$u = u_{RFNN} = \hat{w}^T\hat{\Gamma} + \hat{\delta}\mathrm{sgn}(\mathrm{E^T PB}) \tag{12}$$

where $\hat{w}$, $\hat{m}$, $\hat{\sigma}$, $\hat{r}$ and $\hat{\Gamma}$ are estimations of the optimal parameters, provided by algorithm tuning to be introduced later. Subtracting (12) from (11), an approximation error $\tilde{u}$ is obtained as

$$\begin{aligned}\tilde{u} &= u^* - u = w^{*T}\Gamma^* + \varepsilon - \hat{w}^T\hat{\Gamma} - \hat{\delta}\mathrm{sgn}(\mathrm{E^T PB}) \\ &= \tilde{w}^T\Gamma^* + \hat{w}^T\tilde{\Gamma} + \varepsilon - \hat{\delta}\mathrm{sgn}(\mathrm{E^T PB})\end{aligned} \tag{13}$$

where $\tilde{w} = w^* - \hat{w}$ and $\tilde{\Gamma} = \Gamma^* - \hat{\Gamma}$. The linearization technique transforms the multidimensional receptive-field basis functions into a partially linear form such that the expansion of $\tilde{\Gamma}$ in Taylor series becomes

$$\tilde{\Gamma} = \begin{bmatrix} \tilde{y}_1^3 & \dots & \tilde{y}_9^3 \end{bmatrix}^T = \Gamma_m\tilde{m} + \Gamma_\sigma\tilde{\sigma} + \Gamma_r\tilde{r} + O_v \tag{14}$$

where $\tilde{y}_k^3 = y_k^{3*} - \hat{y}_k^3$, y_k^{3*} the optimal parameter of $\hat{y}_k^3$, $\hat{y}_k^3$ the estimated parameter of y_k^{3*}, $\tilde{m} = m^* - \hat{m}$, $\tilde{\sigma} = \sigma^* - \hat{\sigma}$, $\tilde{r} = r^* - \hat{r}$, O_v higher-order terms, $\Gamma_m = \left[\partial y_1^3/\partial m \ \dots \ \partial y_9^3/\partial m\right]^T|_{m=\hat{m}}$, $\Gamma_\sigma = \left[\partial y_1^3/\partial \sigma \ \dots \ \partial y_9^3/\partial \sigma\right]^T|_{\sigma=\hat{\sigma}}$ and $\Gamma_r = \left[\partial y_1^3/\partial r \ \dots \ \partial y_9^3/\partial r\right]^T|_{r=\hat{r}}$.

Equation (14) can be rewritten as

$$\Gamma^* = \hat{\Gamma} + \Gamma_m\tilde{m} + \Gamma_\sigma\tilde{\sigma} + \Gamma_r\tilde{r} + O_v \tag{15}$$

Substituting (15) into (13), it can be rewritten as:

$$\begin{aligned}\tilde{u} &= \tilde{w}^T(\hat{\Gamma} + \Gamma_m\tilde{m} + \Gamma_\sigma\tilde{\sigma} + \Gamma_r\tilde{r} + O_v) + \hat{w}^T(\Gamma_m\tilde{m} + \Gamma_\sigma\tilde{\sigma} + \Gamma_r\tilde{r} + O_v) + \varepsilon - \hat{\delta}\mathrm{sgn}(\mathrm{E^T PB}) \\ &= \tilde{w}^T\hat{\Gamma} + \hat{w}^T(\Gamma_m\tilde{m} + \Gamma_\sigma\tilde{\sigma} + \Gamma_r\tilde{r}) - \hat{\delta}\mathrm{sgn}(\mathrm{E^T PB}) + D\end{aligned} \tag{16}$$

where $D = \tilde{w}^T(\Gamma_m\tilde{m} + \Gamma_\sigma\tilde{\sigma} + \Gamma_r\tilde{r}) + w^{*T}O_v + \varepsilon$ is the uncertainty term, and this term is assumed to be bounded with a small positive constant δ ($\text{let } |D| \le \delta$). From (1), (4) and (16), an error equation is obtained

$$\begin{aligned}\dot{E} &= AE + B(u^* - u) = AE + B\tilde{u} \\ &= AE + B\left[\tilde{w}^T\hat{\Gamma} + \hat{w}^T(\Gamma_m\tilde{m} + \Gamma_\sigma\tilde{\sigma} + \Gamma_r\tilde{r}) - \hat{\delta}\mathrm{sgn}(\mathrm{E^T PB}) + D\right]\end{aligned} \tag{17}$$

Consider the dynamic system represented by (1), if the RFNNC is designed as (12) with the adaptation laws for networks parameters shown in (18)–(22), the stability of the proposed RFNNC can be guaranteed. where η_1, η_2, η_3, η_4 and η_5 are strictly positive constants.

$$\dot{\hat{w}} = \eta_1 \hat{\Gamma} E^T PB \tag{18}$$

$$\dot{\hat{m}} = \eta_2 \Gamma_m^T \hat{w} E^T PB \tag{19}$$

$$\dot{\hat{\sigma}} = \eta_3 \Gamma_\sigma^T \hat{w} E^T PB \tag{20}$$

$$\dot{\hat{r}} = \eta_4 \Gamma_r^T \hat{w} E^T PB \tag{21}$$

$$\dot{\hat{\delta}} = \eta_5 \left| E^T PB \right| \tag{22}$$

Proof

Define a Lyapunov function candidate as

$$V(t) = \frac{1}{2} E^T PE + \frac{1}{2\eta_1} tr(\tilde{w}^T \tilde{w}) + \frac{1}{2\eta_2} \tilde{m}^T \tilde{m} + \frac{1}{2\eta_3} \tilde{\sigma}^T \tilde{\sigma} + \frac{1}{2\eta_4} \tilde{r}^T \tilde{r} + \frac{1}{2\eta_5} \tilde{\delta}^2 \tag{23}$$

where P is a symmetric positive definite matrix which satisfies the following Lyapunov equation

$$A^T P + PA = -Q \tag{24}$$

where Q is a positive definite matrix. Here, the uncertainty bound estimation error is defined as $\tilde{\delta} = \delta - \hat{\delta}$. Taking the Lyapunov function differential (23) and using (16) and (24), it is concluded that

$$\begin{aligned} \dot{V}(t) = & -\frac{1}{2} E^T QE + E^T PB \left[\tilde{w}^T \hat{\Gamma} + \hat{w}^T (\Gamma_m \tilde{m} + \Gamma_\sigma \tilde{\sigma} + \Gamma_r \tilde{r}) - u_C + D \right] \\ & - \frac{1}{\eta_1} \tilde{w}^T \dot{\hat{w}} - \frac{1}{\eta_2} \dot{\hat{m}}^T \tilde{m} - \frac{1}{\eta_3} \dot{\hat{\sigma}}^T \tilde{\sigma} - \frac{1}{\eta_4} \dot{\hat{r}}^T \tilde{r} - \frac{1}{\eta_5} \tilde{\delta} \dot{\hat{\delta}} \end{aligned} \tag{25}$$

Take (18)-(22) into (25), the derivative of V can be rewritten as

$$\begin{aligned} \dot{V}(t) &= -\frac{1}{2} E^T QE + E^T PBD - E^T PBu_C - \frac{1}{\eta_5} (\delta - \hat{\delta}) \dot{\hat{\delta}} \\ &\le -\frac{1}{2} E^T QE - \left| E^T PB \right| (\delta - |D|) \le 0 \end{aligned} \tag{26}$$

Therefore regardless what the situation is, the derivative of V respect to time is smaller than zero. $\dot{V}(t) \le 0$ is negative semi-definite (i.e., $\dot{V}(t) \le \dot{V}(0)$), which implies E, $\tilde{w}$, $\tilde{m}$, $\tilde{\sigma}$, $\tilde{\delta}$ and $\tilde{r}$ are bounded. Let function $F(t) = E^T QE / 2 \le -\dot{V}(t)$, and integrate function with respect to time.

Because $V(0)$ is bounded, and $V(t)$ is bounded, the following result is obtained:

$$\lim_{t \to \infty} \int_0^t F(\tau) d\tau < \infty \tag{27}$$

Since $\dot{F}(t)$ is bounded, by Barbalat's Lemma it can be shown that $\lim_{t \to \infty} F(t) = 0$. This implies that $E(t)$ will converge to zero as $t \to \infty$. As a result, the stability of the proposed control system can be guaranteed.

2.2 Convergence Analysis of RFNNC

Although the stability of the adaptive RFNNC can be guaranteed, the parameters $\hat{w}$, $\hat{m}$, $\hat{\sigma}$ and $\hat{r}$ in (18)–(21) cannot be guaranteed within a bound value. The RFNNC output is bounded, whether the means, the standard deviation of the Gaussian function and weights are bounded. The constraint sets $\overline{w}$, $\overline{m}$, $\overline{\sigma}$ and $\overline{r}$ are defined respectively

$$U_w = \left\{ \left\| \hat{w} \right\| \le \overline{w} \right\} \tag{28}$$

$$U_m = \left\{ \left\| \hat{m} \right\| \le \overline{m} \right\} \tag{29}$$

$$U_\sigma = \left\{ \left\| \hat{\sigma} \right\| \le \overline{\sigma} \right\} \tag{30}$$

$$U_r = \left\{ \left\| \hat{r} \right\| \le \overline{r} \right\} \tag{31}$$

where $\| \cdot \|$ is a two-norm of vector, $\overline{w}$, $\overline{m}$, $\overline{\sigma}$ and $\overline{r}$ are positive constants, and the adaptive laws (18)-(21) can be modified as follows

$$\dot{\hat{w}} = \begin{cases} \eta_1 \hat{\Gamma} E^T PB, & \text{if } \left\| \hat{w} \right\| < \overline{w} \text{ or } \left(\left\| \hat{w} \right\| = \overline{w} \text{ and } E^T PB\hat{w}^T \hat{\Gamma} \le 0 \right) \\ \eta_1 \hat{\Gamma} E^T PB - \eta_1 \hat{\Gamma} E^T PB \dfrac{\hat{w}\hat{w}^T}{\left\| \hat{w} \right\|^2}, & \text{if } \left\| \hat{w} \right\| = \overline{w} \text{ and } E^T PB\hat{w}^T \hat{\Gamma} > 0 \end{cases} \tag{32}$$

$$\dot{\hat{m}} = \begin{cases} \eta_2 \Gamma_m^T \hat{w} E^T PB, & \text{if } \left\| \hat{m} \right\| < \overline{m} \text{ or } \left(\left\| \hat{m} \right\| = \overline{m} \text{ and } E^T PB\hat{w}^T \Gamma_m \hat{m} \le 0 \right) \\ \eta_2 \Gamma_m^T \hat{w} E^T PB - \eta_2 \Gamma_m^T \hat{w} E^T PB \dfrac{\hat{m}\hat{m}^T}{\left\| \hat{m} \right\|^2}, & \text{if } \left\| \hat{m} \right\| = \overline{m} \text{ and } E^T PB\hat{w}^T \Gamma_m \hat{m} > 0 \end{cases} \tag{33}$$

$$\dot{\hat{\sigma}} = \begin{cases} \eta_3 \Gamma_\sigma^T \hat{w} E^T PB, & \text{if } \left\| \hat{\sigma} \right\| < \overline{\sigma} \text{ or } \left(\left\| \hat{\sigma} \right\| = \overline{\sigma} \text{ and } E^T PB\hat{w}^T \Gamma_\sigma \hat{\sigma} \le 0 \right) \\ \eta_3 \Gamma_\sigma^T \hat{w} E^T PB - \eta_3 \Gamma_\sigma^T \hat{w} E^T PB \dfrac{\hat{\sigma}\hat{\sigma}^T}{\left\| \hat{\sigma} \right\|^2}, & \text{if } \left\| \hat{\sigma} \right\| = \overline{\sigma} \text{ and } E^T PB\hat{w}^T \Gamma_\sigma \hat{\sigma} > 0 \end{cases} \tag{34}$$

$$\dot{\hat{r}} = \begin{cases} \eta_4 \Gamma_r^T \hat{w} E^T PB, & \text{if } \left\| \hat{r} \right\| < \overline{r} \text{ or } \left(\left\| \hat{r} \right\| = \overline{r} \text{ and } E^T PB\hat{w}^T \Gamma_r \hat{r} \le 0 \right) \\ \eta_4 \Gamma_r^T \hat{w} E^T PB - \eta_4 \Gamma_r^T \hat{w} E^T PB \dfrac{\hat{r}\hat{r}^T}{\left\| \hat{r} \right\|^2}, & \text{if } \left\| \hat{r} \right\| = \overline{r} \text{ and } E^T PB\hat{w}^T \Gamma_r \hat{r} > 0 \end{cases} \tag{35}$$

If the initial values $\hat{w}(0) \in U_w$, $\hat{m}(0) \in U_m$, $\hat{\sigma}(0) \in U_\sigma$ and $\hat{r}(0) \in U_r$ then the adaptive laws (32)-(35)guarantee that $\hat{w}(t) \in U_w$, $\hat{m}(t) \in U_m$, $\hat{\sigma}(t) \in U_\sigma$ and $\hat{r}(t) \in U_r$ for all $t \ge 0$.

Define a Lyapunov function as

$$v_w = \frac{1}{2} \hat{w}^T \hat{w} \tag{36}$$

The derivative of the Lyapunov function is presented as

$$\dot{v}_w = \hat{w}^T \dot{\hat{w}} \tag{37}$$

Assume the first line of (32) is true, either $\left\| \hat{w} \right\| < \overline{w}$ or $\left(\left\| \hat{w} \right\| = \overline{w} \text{ and } E^T PB\hat{w}^T \hat{\Gamma} \le 0 \right)$. Substituting the first line of (32) into (37), which becomes $\dot{v}_w = \eta_1 E^T PB\hat{w}^T \hat{\Gamma} \le 0$. As a

result, $\|\hat{w}\| \le \bar{w}$ is guaranteed. In addition, when $\|\hat{w}\| = \bar{w}$ *and* $E^T PB\hat{w}^T\hat{\Gamma} > 0$, $\dot{v}_w = \eta_1 E^T PB\hat{w}^T\hat{\Gamma} - \eta_1 E^T PB\dfrac{\hat{w}^T\hat{w}}{\|\hat{w}\|^2}\hat{w}^T\hat{\Gamma} = 0$. That $\|\hat{w}\| \le \bar{w}$ can be also assured. Thereby, the initial value of $\hat{w}$ is bounded, $\|\hat{w}\|$ is bounded by the constraint set $\bar{w}$ for $t \ge 0$. Similarly, it can be proved that $\|\hat{m}\|$ is bounded by the constraint set $\bar{m}$, $\|\hat{\sigma}\|$ is bounded by the constraint set $\bar{\sigma}$ and $\|\hat{r}\|$ is bounded by the constraint set $\bar{r}$ for $t \ge 0$.

When the condition $\|\hat{w}\| < \bar{w}$ or $\left(\|\hat{w}\| = \bar{w}\ and\ E^T PB\hat{w}^T\hat{\Gamma} \le 0\right)$, $\|\hat{m}\| < \bar{m}$ or $\left(\|\hat{m}\| = \bar{m}\ and\ E^T PB\hat{w}^T\Gamma_m\hat{m} \le 0\right)$, $\|\hat{\sigma}\| < \bar{\sigma}$ or $\left(\|\hat{\sigma}\| = \bar{\sigma}\ and\ E^T PB\hat{w}^T\Gamma_\sigma\hat{\sigma} \le 0\right)$, $\|\hat{r}\| < \bar{r}$ or $\left(\|\hat{r}\| = \bar{r}\ and\ E^T PB\hat{w}^T\Gamma_r\hat{r} \le 0\right)$, the stability analysis the same as (33), (34) and (35). In the other situation, the condition $\|\hat{w}\| = \bar{w}$ and $E^T PB\hat{w}^T\hat{\Gamma} > 0$, $\|\hat{m}\| = \bar{m}$ and $E^T PB\hat{w}^T\Gamma_m\hat{m} > 0$, $\|\hat{\sigma}\| = \bar{\sigma}$ and $E^T PB\hat{w}^T\Gamma_\sigma\hat{\sigma} > 0$, $\|\hat{r}\| = \bar{r}$ and $E^T PB\hat{w}^T\Gamma_r\hat{r} > 0$ is occurred, the Lyapunov function can be rewritten as follows

$$\begin{aligned}
\dot{v}_w &= -\frac{1}{2}E^T QE + E^T PB\left(\tilde{w}^T\hat{\Gamma} + \hat{w}^T\Gamma_m\tilde{m} + \hat{w}^T\Gamma_\sigma\tilde{\sigma} + \hat{w}^T\Gamma_r\tilde{r}) + D - u_C\right) - \frac{1}{\eta_1}\tilde{w}^T\dot{\hat{w}} \\
&\quad - \frac{1}{\eta_2}\dot{\hat{m}}^T\tilde{m} - \frac{1}{\eta_3}\dot{\hat{\sigma}}^T\tilde{\sigma} - \frac{1}{\eta_4}\dot{\hat{r}}^T\tilde{r} - \frac{1}{\eta_5}\tilde{\delta}\dot{\hat{\delta}} \\
&= -\frac{1}{2}E^T QE + E^T PB\left(D - u_C\right) + E^T PB\frac{\tilde{w}^T\hat{w}}{\|\hat{w}\|^2}\hat{w}^T\hat{\Gamma} + (\Gamma_m^T\hat{w})^T E^T PB\hat{m}\frac{\hat{m}^T\tilde{m}}{\|\hat{m}\|^2} \\
&\quad + (\Gamma_\sigma^T\hat{w})^T E^T PB\hat{\sigma}\frac{\hat{\sigma}^T\tilde{\sigma}}{\|\hat{\sigma}\|^2} + (\Gamma_r^T\hat{w})^T E^T PB\hat{r}\frac{\hat{r}^T\tilde{r}}{\|\hat{r}\|^2} - \frac{1}{\eta_5}\tilde{\delta}\dot{\hat{\delta}}
\end{aligned} \tag{38}$$

Equation $\tilde{w}^T\hat{w} = \left(\|w^*\|^2 - \|\hat{w}\|^2 - \|\tilde{w}\|^2\right)/2 < 0$, which is according to $\|\hat{w}\| = \bar{w} > \|\hat{w}^*\|$. Similarly, $\|\hat{m}\| = \bar{m} > \|\hat{m}^*\|$, $\|\hat{\sigma}\| = \bar{\sigma} > \|\hat{\sigma}^*\|$ and $\|\hat{r}\| = \bar{r} > \|\hat{r}^*\|$ can be proven. It is finally obtained as

$$\begin{aligned}
\dot{v}_w &= -\frac{1}{2}E^T QE + E^T PBD - E^T PBu_C + E^T PB\frac{\tilde{w}^T\hat{w}}{\|\hat{w}\|^2}\hat{w}^T\hat{\Gamma} + \Gamma_m^T\hat{w}E^T PB\hat{m}\frac{\hat{m}^T\tilde{m}}{\|\hat{m}\|^2} \\
&\quad + \Gamma_\sigma^T\hat{w}E^T PB\hat{\sigma}\frac{\hat{\sigma}^T\tilde{\sigma}}{\|\hat{\sigma}\|^2} + \Gamma_r^T\hat{w}E^T PB\hat{r}\frac{\hat{r}^T\tilde{r}}{\|\hat{r}\|^2} - \frac{1}{\eta_5}\tilde{\delta}\dot{\hat{\delta}} \\
&\le -\frac{1}{2}E^T QE + E^T PB\frac{\left(\|w^*\|^2 - \|\hat{w}\|^2 - \|\tilde{w}\|^2\right)}{\|\hat{w}\|^2}\hat{w}^T\hat{\Gamma} \\
&\quad + \frac{1}{2}(\Gamma_m^T\hat{w})^T E^T PB\hat{m}\frac{\left(\|m^*\|^2 - \|\hat{m}\|^2 - \|\tilde{m}\|^2\right)}{\|\hat{m}\|^2} \\
&\quad + \frac{1}{2}(\Gamma_\sigma^T\hat{w})^T E^T PB\hat{\sigma}\frac{\left(\|\sigma^*\|^2 - \|\hat{\sigma}\|^2 - \|\tilde{\sigma}\|^2\right)}{\|\hat{\sigma}\|^2} \\
&\quad + \frac{1}{2}(\Gamma_r^T\hat{w})^T E^T PB\hat{r}\frac{\left(\|r^*\|^2 - \|\hat{r}\|^2 - \|\tilde{r}\|^2\right)}{\|\hat{r}\|^2} \\
&\le -\frac{1}{2}E^T QE \le 0
\end{aligned} \tag{39}$$

Using the same discussion shown in the previous section, the stability property can also be guaranteed since $E \to 0$ as $t \to 0$.

2.3 General Regression Neural Networks Controller

As a common nonlinear problem, a dead-zone often appears in the control system, which not only makes a steady-sate error, it also deteriorates the dynamic quality of the control systems. The GRNNC is proposed to solve this problem. The GRNNC is a powerful regression tool with a dynamic network structure and the training speed is extremely fast. Due to the simplicity of the network structure and ease of implementation, it can be widely applied to a variety of fields.

The GRNNC structure, shown in Fig. 3, is suggested for the system input nonlinear compensation. The input u is the RFNNC output, W_G^1 is the weight of the hidden layer, W_G^2 is the weight of the output layer, a is the output of the hidden layer, u_G is the output of the output layer.

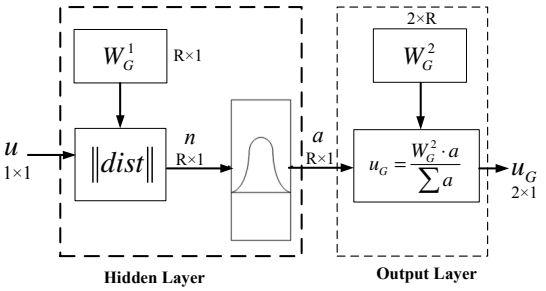

Fig. 3. The GRNNC structure

The GRNNC is composed of two layers, the hidden layer and the output layer. The input u of the GRNNC means a torque calculated by the RFNNC. The outcome n of $\|dist\|$ represents the Euclidean distance between the input u and each element of W_G^1. n is passed using a Gaussian function. When the Euclidean distance between u and W_G^1 is far, the output element a approaches zero. On the other hand, if the Euclidean distance is short the output element a approaches one. The Gaussian function is

$$a = \exp\left(-\left(\frac{n-m}{\sigma}\right)^2\right) \tag{40}$$

where m and σ are the center and standard deviation of the Gaussian function, respectively. In order to increase the discrimination and have better performance, the standard deviation σ value of the Gaussian function is chosen as low.

The relation function of the output layer can be expressed as

$$u_G = \frac{W_G^2 \cdot a}{\sum a} \tag{41}$$

The output vector of the hidden layer a is multiplied with appropriate weights W_G^2 to sum up the output u_G of the GRNNC. The output u_G is composed of frequency control u_f and phase control u_P and expressed as

$$u_G = \begin{bmatrix} u_f & u_p \end{bmatrix}^T \tag{42}$$

Applying the GRNNC, the dead-zone of the TWUSM will be compensated as desired.

3 Experiments

Experiments are required to prove the feasibility of the proposed scheme. Figure 4 shows the experimental structure, which includes TMS320F2812 digital signal processor (DSP), TWUSM driver and TWUSM. The TMS320F2812 DSP experiment board is applied as the computing core. The DSP program was coded in C language. After compilation, assembly and link, the execution file is generated by C2000 code composer (CCS). The execution file is executed in the same windows interface.

In these experiments three different controllers were chosen for comparison.

(i) The proposed control scheme, RFNNC and GRNNC.

(ii) The RFNNC only, without GRNNC. The control algorithm of RFNNC only is the same as RFNNC of the proposed control scheme.

(iii) The PI controller. The PI controller is the one of the most used controller in linear system. The control PI controller has important advantages such as a simple structure and easy to design. Therefore, PI controllers are used widely in industrial applications. Owing to the absence of the TWUSM mathematical model, the PI controller parameters are chosen by trial and error in such a way that the optimal performance occurs at rated conditions. A block diagram of the angle control system for an ultrasonic motor using a PI controller is shown in Fig. 5. Where θ_r and θ are the command and rotor angle, *e(k)* is the tracking error, u_f is the frequency command, u_p is the phase different command, respectively. The PI controller parameters were selected as $K_P = 1000$ and $K_I = 100$.

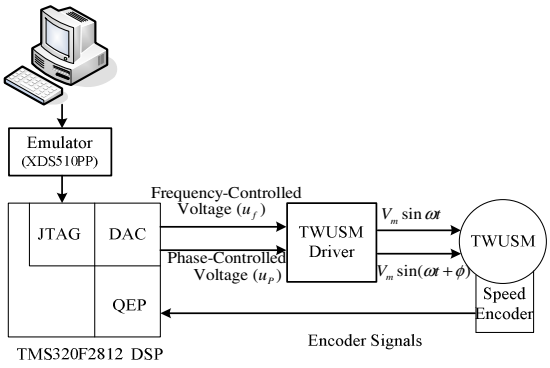

Fig. 4. The experiment structure

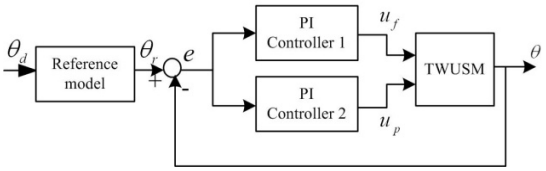

Fig. 5. The block diagram of the dual-mode PI control

Figures 6 to 8 show the experimental results for the proposed control scheme, the RFNNC only, and the PI control respectively, for a periodic square angle command from -90 to 90 degrees. Figures 9 to 11 show the experimental results for the proposed control scheme, the RFNNC only, and the PI control respectively, for a sinusoidal angle command from -90 to 90 degrees. Figure (a) shows the TWUSM angle response and speed response. Figure (b) shows the angle error between angle command and angle response.

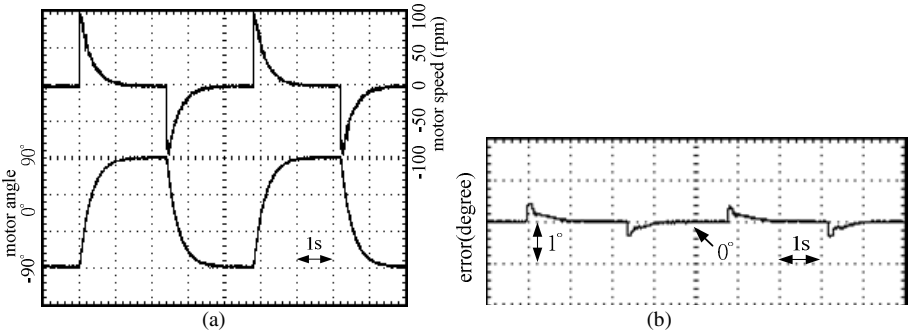

Fig. 6. The experimental result for the proposed control scheme for a periodic angle square command from -90 to 90 degrees

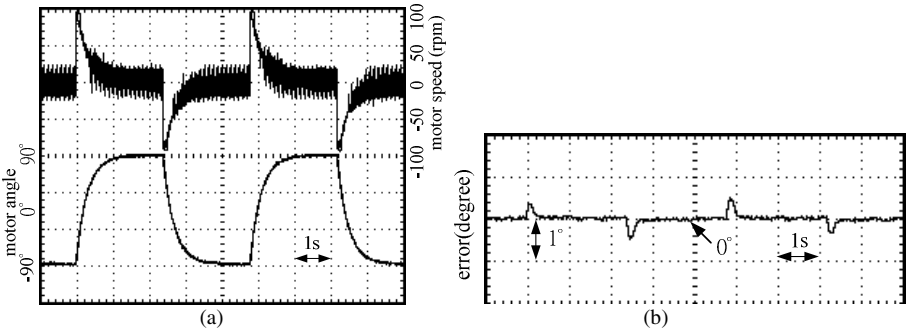

Fig. 7. The RFNNC only experimental result for a periodic square angle command from -90 to 90 degrees

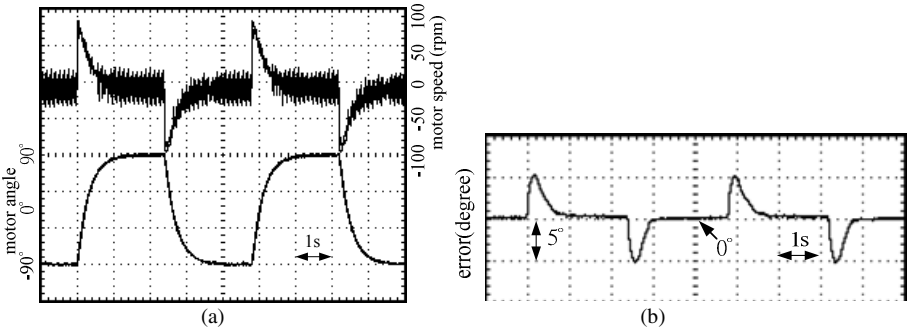

Fig. 8. The experimental result for the PI control for a periodic square angle command from -90 to 90 degrees

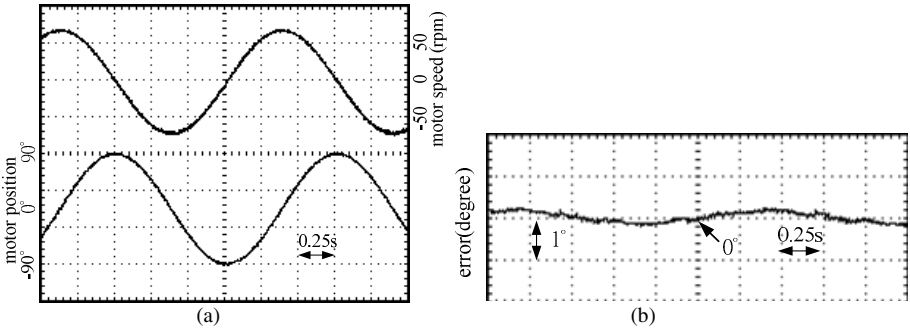

Fig. 9. The experimental result for the proposed control scheme for a sinusoidal angle command from -90 to 90 degrees

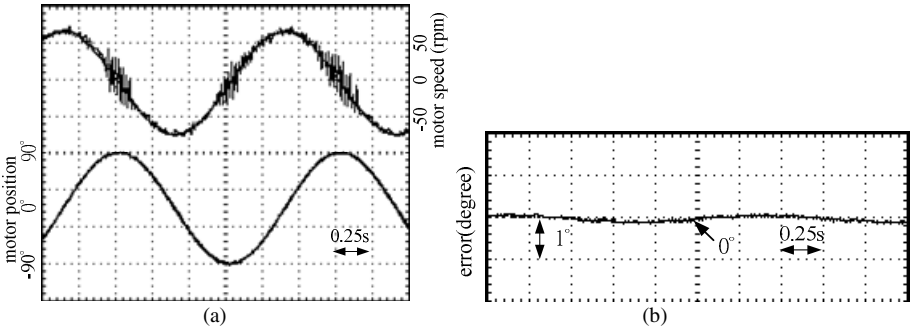

Fig. 10. The RFNNC only experimental result for a sinusoidal angle command from -90 to 90 degrees

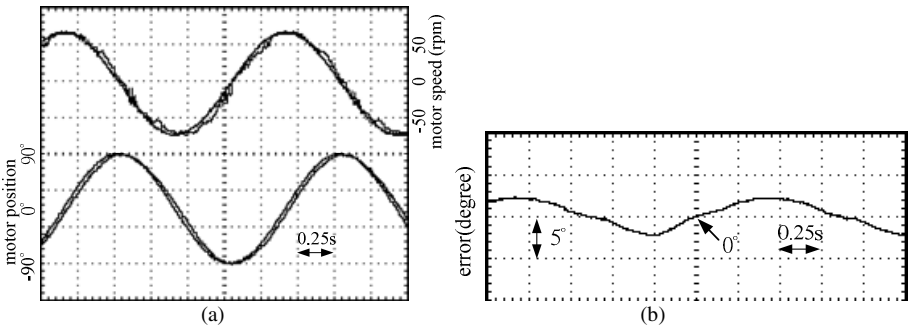

Fig. 11. The experimental result for the PI control for a sinusoidal angle command from -90 to 90 degrees

Observing the experimental results for the proposed control scheme in Figs. 6 and 9 the tracking errors for both can converge to an acceptable region and the control performance is excellent. The proposed controller retains control performance and has no dead-zone.

The RFNNC only experimental results in Figs. 7 and 10 show that the tracking error is similar to the proposed control scheme. However, the RFNNC drawbacks interfere with the dead-zone and the motor speed has a serious chattering phenomenon at slow speed near zero.

Figures 8 and 11 illustrate that the PI controller has a chattering phenomenon like the RFNNC only and a larger tracking error.

4 Conclusions

This paper presented a proposed control scheme, RFNNC and GRNNC, applied to the TWUSM. Many concepts such as controller design and the stability analysis of the controller are introduced. The experiment results show that the proposed control scheme is feasible and the performance is better than conventional control methods.

The proposed control scheme includes the RFNNC and GRNNC. The RFNNC is designed to track the reference angle. The membership function and weight variables can be updated using adaptive algorithms. Moreover, all parameters proposed RFNNC parameters are tuned in the Lyapunov sense; thus, the system stability can be guaranteed. In the RFNNC a compensated controller is designed to recover the residual part of the approximation error. The GRNNC is appended to the RFNNC to compensate for the TWUSM system dead zone using a predefined set. The GRNNC can successfully avoid the TWUSM dead-zone problem. The experimental results verify that the proposed controller can control the system well.

Acknowledgements. The authors would like to express their appreciation to NSC for supporting under contact NSC 97-2221-E-168 -050 -MY3.

References

1. Sashida, T., Kenjo, T.: An introduction to ultrasonic motors. Clarendon Press, Oxford (1993)
2. Ueha, S., Tomikawa, Y.: Ultrasonic motors theory and applications. Clarendon Press, Oxford (1993)
3. Uchino, K.: Piezoelectric actuators and ultrasonic motors. Kluwer Academic Publishers (1997)
4. Huafeng, L., Chunsheng, Z., Chenglin, G.: Precise position control of ultrasonic motor using fuzzy control with dead-zone compensation. J. of Electrical Engineering 56(1-2), 49–52 (2005)
5. Uchino, K.: Piezoelectric ultrasonic motors: overview. Smart Materials and Structures 7, 273–285 (1998)
6. Chen, T.C., Yu, C.H., Tsai, M.C.: A novel driver with adjustable frequency and phase for travelling-wave type ultrasonic motor. Journal of the Chinese Institute of Engineers 31(4), 709–713 (2008)
7. Hagood, N.W., Mcfarland, A.J.: Modeling of a piezoelectric rotary ultrasonic motor. IEEE Trans. on Ultrasonics, Ferroelectrics, and Frequency Control 42(2), 210–224 (1995)
8. Bal, G., Bekiroglu, E.: Servo speed control of travelling-wave ultrasonic motor using digital signal processor. Sensor and Actuators A 109, 212–219 (2004)
9. Bal, G., Bekiroglu, E.: A highly effective load adaptive servo drive system for speed control of travelling-wave ultrasonic motor. IEEE Trans. on Power Electronics 20(5), 1143–1149 (2005)
10. Alessandri, A., Cervellera, C., Sanguineti, M.: Design of asymptotic estimators: an approach based on neural networks and nonlinear programming. IEEE Trans. on Neural Networks 18(1), 86–96 (2007)
11. Liu, M.: Delayed standard neural network models for control systems. IEEE Trans. on Neural Networks 18(5), 1376–1391 (2007)
12. Abiyev, R.H., Kaynak, O.: Fuzzy wavelet neural networks for identification and control of dynamic plants-A novel structure and a comparative study. IEEE Trans. on Industrial Electronics 55(8), 3133–3140 (2008)
13. Lin, C.M., Hsu, C.F.: Recurrent neural network based adaptive -backstepping control for induction servomotors. IEEE Trans. on Industrial Electronics 52(6), 1677–1684 (2005)
14. Ku, C.C., Lee, K.Y.: Diagonal recurrent neural networks for dynamic systems control. IEEE Trans. on Neural Networks 6(1), 144–156 (1995)
15. Juang, C.F., Huang, R.B., Lin, Y.Y.: A recurrent self-evolving interval type-2 fuzzy neural network for dynamic system processing. IEEE Trans. on Fuzzy Systems 17(5), 1092–1105 (2009)
16. Stavrakouds, D.G., Theochairs, J.B.: Pipelined recurrent fuzzy neural networks for nonlinear adaptive speech prediction. IEEE Trans. on Systems, Man and Cybernetics, Part B 37(5), 1305–1320 (2007)
17. Lin, C.J., Chen, C.H.: Identification and prediction using recurrent compensatory neuro-fuzzy systems. Fuzzy Sets and Systems 150(2), 307–330 (2005)
18. Senjyu, T., Kashiwagi, T., Uezato, K.: Position control of ultrasonic motors using MRAC with deadzone compensation. IEEE Trans. on Power Electronics 17(2), 265–272 (2002)